Ecosystem Indicators and Trends Used by FOCI - 2004
Edited by S. Allen Macklin, NOAA/PMEL

FOCI's scientists employ a number of climate, weather, and ocean indices and trends to help describe and ascribe the status of the ecosystem to various patterns or regimes. This document presents some of these with respect to current (2004) conditions. This section begins with an overview of North Pacific climate for 2004, including an examination of trends and tendencies in multidecadal and decadal climate regimes. Following this section are sections dealing explicitly with the western Gulf of Alaska and eastern Bering Sea. Within these are continuations of discussions begun in 2003 on eddy kinetic energy in the Gulf of Alaska and modeled drift trajectories for the Bering Sea.

North Pacific Climate Overview – FOCI
S. Rodionov, J. Overland, and N. Bond (NOAA/PMEL)

Summary. *The purpose of this report is to provide a summary of recent atmosphere-ocean conditions in the North Pacific in the context of its primary modes of variability. The first part of this report is focused on decadal-scale variability after the major climate shift in the late 1970s, and the second part describes the climate conditions in 2004. It is shown that in the past three decades the North Pacific climate system experienced two minor regime shifts. The first of these shifts occurred in 1989, primarily in the winter Pacific Decadal Oscillation (PDO) index, which represents the leading mode of North Pacific sea surface temperature (SST) variability and is related to the strength of the Aleutian low. The second shift was in 1998, and was associated with a change in the sign of the second principal mode of North Pacific SST variability, the so-called Victoria pattern, in winter and the PDO index in summer. The atmospheric expression of the Victoria pattern is a north-south pressure dipole, with the negative 500-hPa height anomaly center over the eastern Aleutian Islands and the positive center over the east-central North Pacific (positive mode of the pattern). During the period 1989-1997, atmospheric pressure tended to be above normal in the high latitudes and below normal in the mid-latitudes, which translated to a relative cooling in the Bering Sea. Since 1998, the polarity of the winter north-south pressure dipole reversed. The SST field in the eastern Bering Sea became anomalously warm, whereas colder-than-normal conditions were established along the U.S. West Coast. During the summer season, the 1998 shift exhibited itself in a transition from the north-south pressure dipole to a monopole characteristic of the negative PDO pattern. It is unclear whether this shift in the summer PDO index to significantly negative values from 1999 through 2001 represents just a temporary reprieve from positive PDO conditions, or heralds the onset of an extended period featuring negative PDO conditions throughout the year.*

Recent Regime Shifts on the Decadal Time Scale

The climate shift that occurred in the late 1970s was associated with an abrupt transition from a negative to a positive phase of the Pacific Decadal Oscillation (PDO). The PDO index tracks major, multidecadal changes in the North Pacific climate, often referred to as regimes (Mantua et al. 1997). In addition to these multidecadal regimes, the climate

experiences minor, decadal-scale regimes. Minobe (1999) discusses a possible resonance between the regimes on these two time scales, which may lead to an amplification of the magnitude of a shift as in the mid-1940s and late 1970s.

A question critically important for fisheries is whether a string of negative values of the PDO index in the late 1990s and early 2000s signifies the end of the positive PDO regime established in the late 1970s, or if it was just a temporary deviation from that regime, possibly associated with the prolonged La Niña event of 1998-2001. If this is a climate regime shift, is it on the decadal or longer time scale? It is also possible that recent changes in the North Pacific climate have little to do with the PDO, which is the first principal mode of sea surface temperature (SST) variability, but rather with the Victoria pattern, which is its second principal mode (Overland et al. 2004).

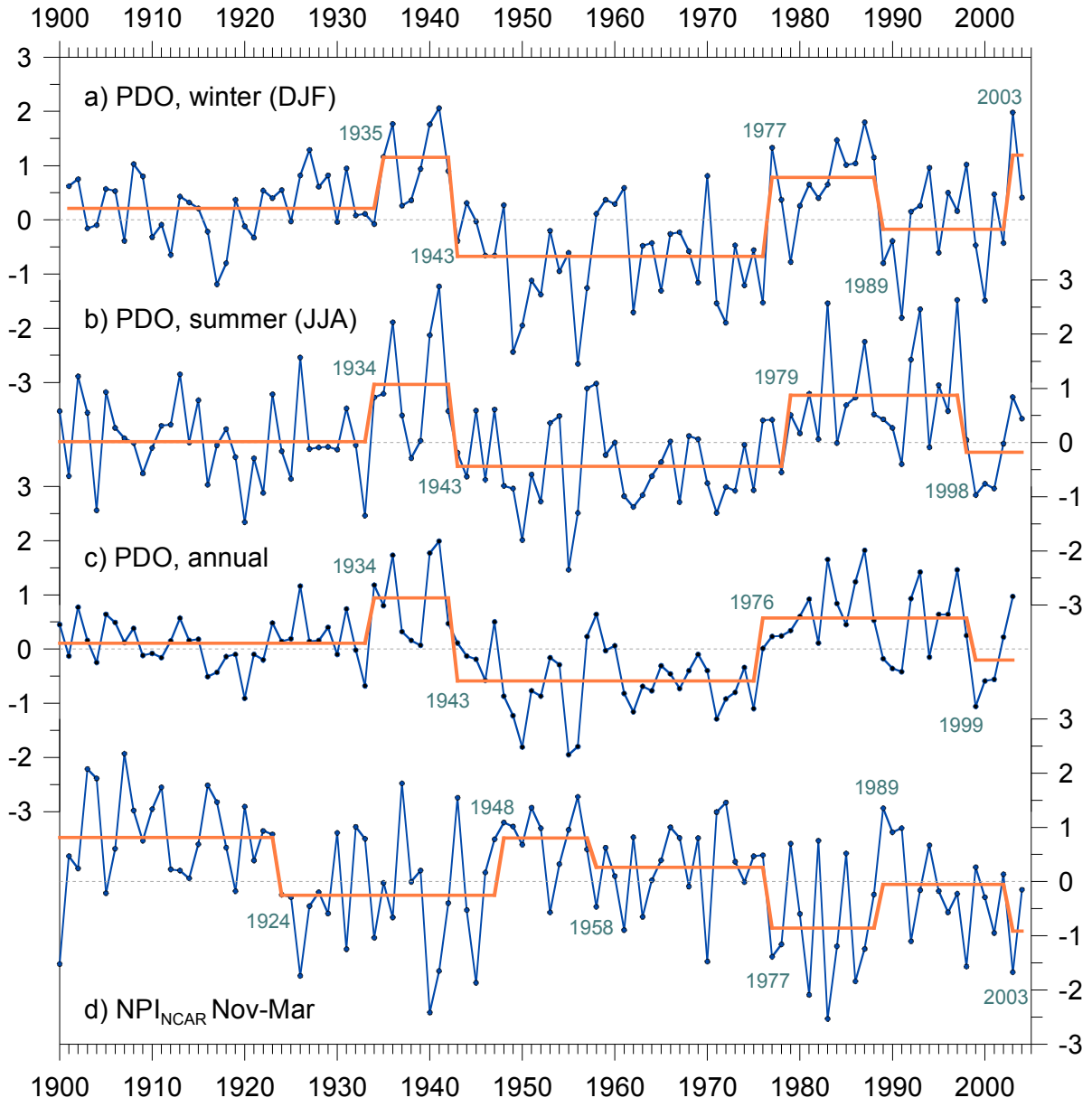

Figure 16. a) Mean winter (DJF) PDO index, 1901-2004, b) mean summer (JJA) PDO index, 1900-2004, c) Annual (Jan-Dec) PDO index, 1900-2003, and d) North Pacific index (Nov-Mar) from the National Center for Atmospheric Research (Trenberth and Hurrell 1994), 1900-2004. The stepwise functions (orange lines) characterize regime shifts in the level of fluctuations of the indices. Shift points were calculated using the STARS method (Rodionov 2004), with the cutoff length of 10 years and significance levels of 0.05 for the PDO indices and 0.2 for the NPI_{NCAR} index.

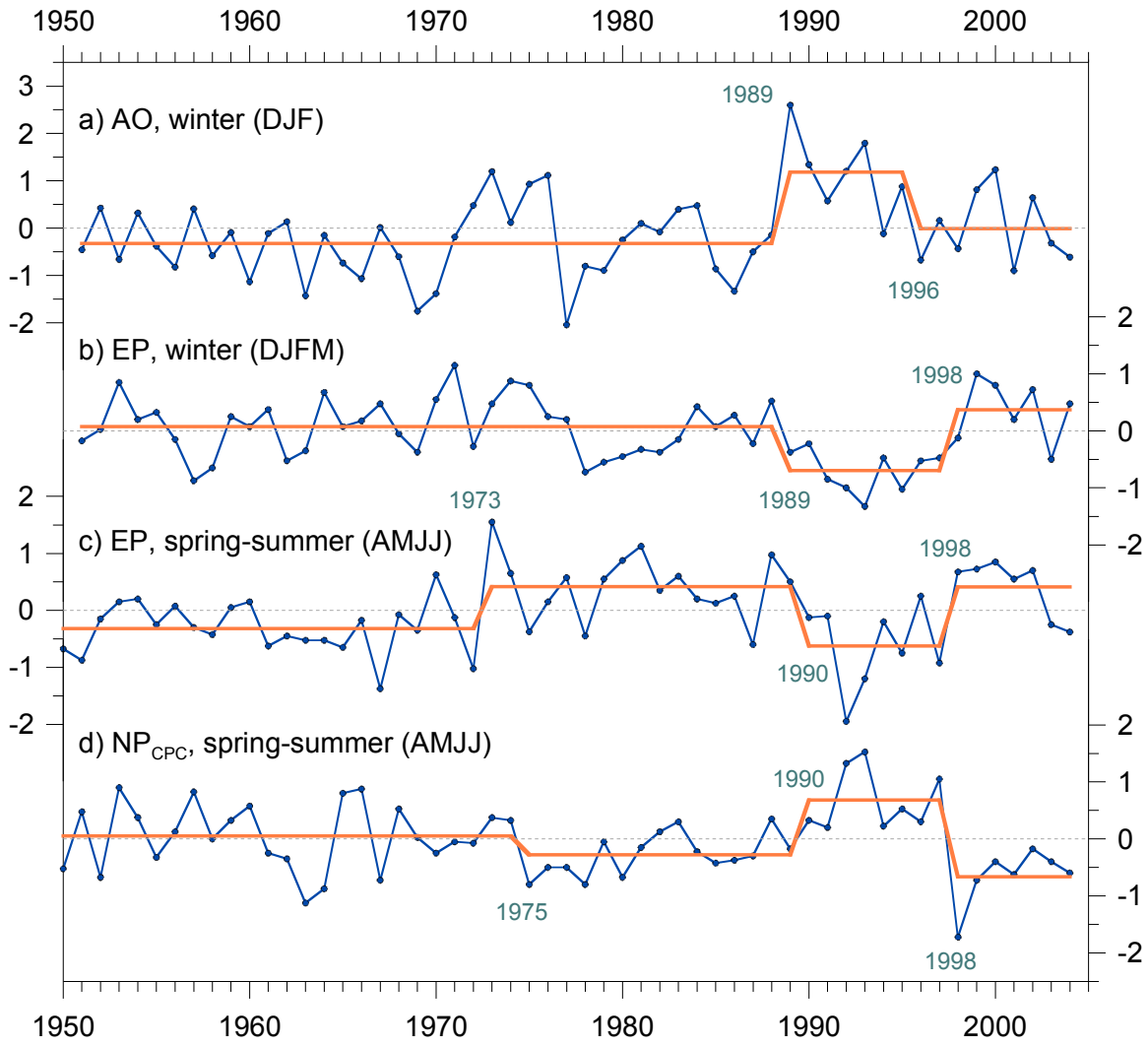

Figure 17. a) Mean winter (DJF) Arctic Oscillation index, 1951-2004, b) mean winter (DJFM) East Pacific index, 1951-2004, c) Mean spring-summer (AMJJ) East Pacific index, 1950-2004, and d) mean spring-summer (AMJJ) North Pacific index from the Climate Prediction Center, 1950-2003. The stepwise functions (orange lines) characterize regime shifts in the level of fluctuations of the indices. Shift points were calculated using the STARS method (Rodionov 2004), with the cutoff length of 10 years and significance levels of 0.1 for the NPI_{CPC} index and 0.05 for other indices.

A regime shift analysis of the mean winter (DJF) PDO time series using the STARS method (Rodionov 2004) reveals only two regime shifts that are significant at the 0.01 level, one in 1943 and the other one in 1977. At the 0.05 level, however, the shift in 1989 is also detected (Figure 16). The magnitude of the 1989 shift was not as large as the one in 1977. Nevertheless, it survived the test, despite a series of positive PDO values in the mid-1990s. Having analyzed 100 physical and biological time series, Hare and Mantua (2000) came to conclusion that the regime shift of 1989 was not as persuasive as the 1977 shift; it was more prominent in biological records than in indices of Pacific climate (McFarlane 2000). In 2003, the winter PDO index was the highest since 1941. This suggests a possibility of a new regime shift; however, it may be just a reaction to the El Niño event of 2002-2003. The shift of 1989 and a possible shift in 2003 can also be seen

in the North Pacific (NP) index (Trenberth and Harrell 1994), albeit at the less strict significance level (0.2) due to strong interannual variability in the index (Figure 16d).

The pattern of temporal variability for the summer (Figure 16b) and annual (Figure 16c) PDO indices is different from that for the winter PDO index. The negative index values in the late 1980s and early 1990s were not large enough to qualify as a regime shift. Instead, a regime shift was detected in the late 1990s. During the past 7 years (1998-2004), the values of the summer PDO index were lower than the average value of the index for the regime of 1979-1997.

The shifts of 1989 and 1998 can be found in other climatic indices as well. One of the most noticeable manifestations of the 1989 shift was an abrupt transition from a negative phase of the Arctic Oscillation (AO) index to its positive phase (Figure 17a). When the AO index is in its positive phase, it usually translates into positive sea level pressure (SLP) anomalies over the North Pacific and the Bering Sea. In fact, the mean winter Bering Sea pressure index (see the Bering Sea section of this report) shows a marked increase in SLP during the period 1989-1997. At the same time, the 1990s were characterized by frequent El Niño events and an elevated SST background in the equatorial Pacific. The period 1990-1995 has been considered as one continuous El Niño event (Trenberth and Hoar 1995), which was soon followed by the extremely strong El Niño event of 1997-1998. During El Niño events, the Aleutian low typically is stronger (deeper) than normal and is displaced south-east of its normal position (Niebauer 1998). The result of this combined effect of the AO and ENSO was a north-south pressure dipole over the eastern North Pacific, both in SLP (not shown) and 500-hPa height anomalies (Figure 18a). This dipole is the atmospheric expression of what Overland et al. (2004) call the Victoria pattern. The oceanic part of the pattern is the second principal mode of SST variability in the North Pacific that will be described below.

The Victoria pattern is related to a teleconnection mode previously identified by correlation and principal component analyses, the East Pacific (EP) pattern. The EP pattern is a north-south dipole which in its positive phase has a negative 500-hPa height anomaly center in the Gulf of Alaska and a positive center in the east-central North Pacific. During the period 1990-1997, the EP index was persistently negative (Figure 17b). The distribution of correlation coefficients between the EP index and SSTs (Figure 19a) clearly resembles the second principal mode of the North Pacific SST variability described by Bond et al. (2003). Unlike the PDO pattern (Figure 19b), for which SST anomalies have the same sign along the entire west coast of North America, the second SST mode features anomalies of one sign along the U.S. West Coast and of opposite sign in the Gulf of Alaska and eastern Bering Sea. For the latter region, the 1990s were a relatively cold period.

Starting with the winter of 1998, the EP became predominantly positive (Figure 17b), i.e., the polarity of the north-south pressure dipole switched (Figure 18b). As a whole, the period 1998-2004 was characterized by an increased cyclonic activity in the Bering Sea and anomalously strong Subtropical high. The only exception from this pattern was the El Niño winter of 2003 when the EP index was negative due to a strongly negative 500-hPa

height anomaly in the east-central North Pacific. The SST response to these atmospheric changes, as it can be inferred from Figure 18a, was a switch toward notably colder winters in the California Current region (Peterson and Schwing 2003) and a string of anomalously mild winters in the Bering Sea (Bond et al. 2003).

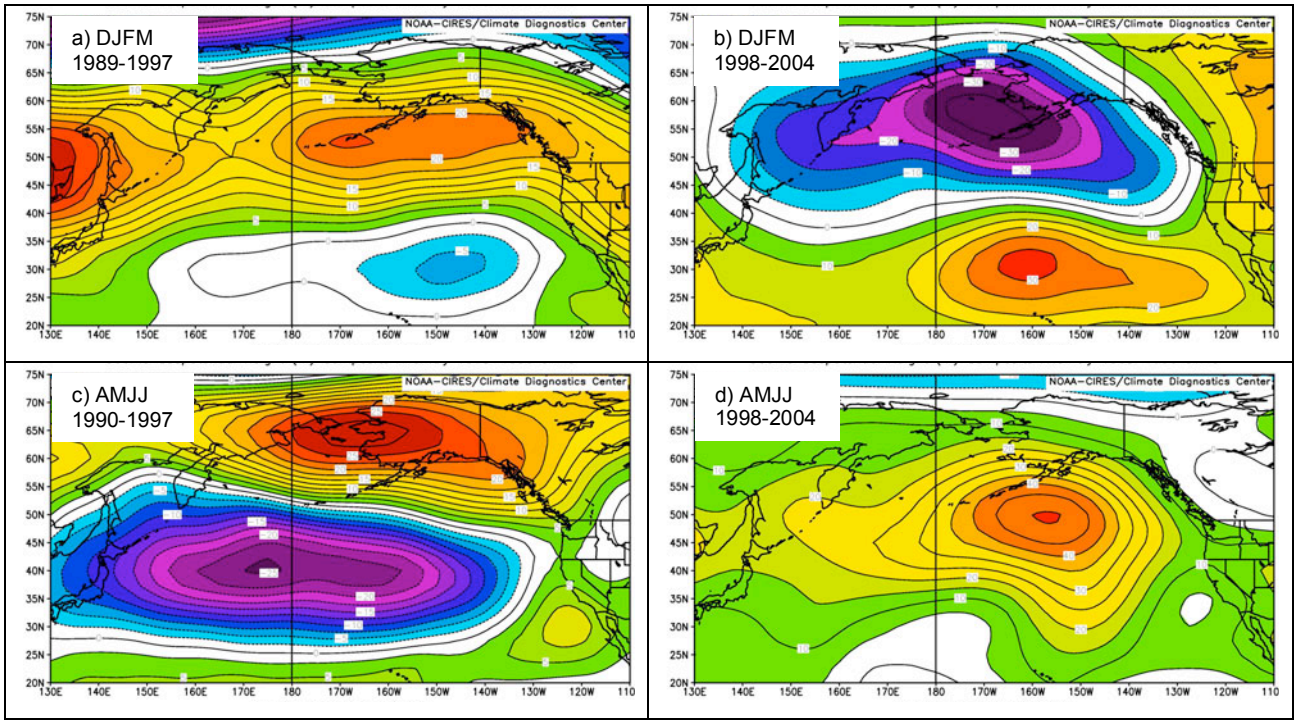

Figure 18. 500-hPa height composite anomalies in winter (DJFM) of a) 1989-1997 and b) 1998-2004 and spring-summer (AMJJ) of c) 1990-1997 and d) 1998-2004. The base period for calculating anomalies is 1968-1996.

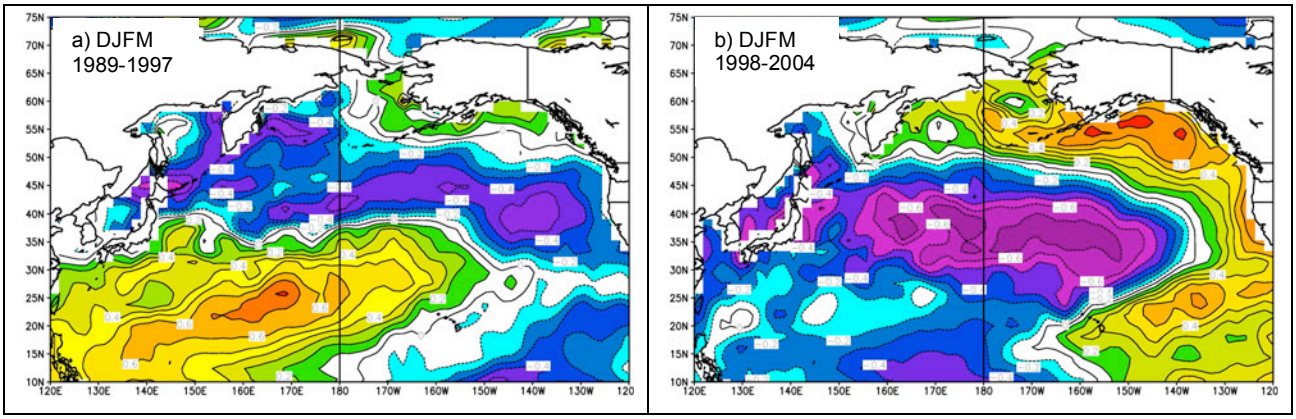

Figure 19. The distribution of the correlation coefficients between a) the EP index and b) the PDO index and SST anomalies for the winter (DJFM) season, 1982-2004.

The 1998 regime shift exhibited itself strongly in spring-summer months as well, as evidenced by the EP index and North Pacific (NP_{CPC}) indices for April-July (Figures 17c and 17d, respectively). Positive values of the NP_{CPC} index correspond to higher 500-hPa heights over the Bering Sea and lower heights for the region south of the Aleutian Islands. Therefore, during the period 1990-1997, the north-south pressure dipole was basin wide (Figure 18c) and not limited to the eastern North Pacific as in winter (Figure 18a). In spring-summer, the shift of 1998 was characterized not by a shift in the polarity of the north-south pressure dipole as in winter, but by a transition to a monopole with a high pressure center south of the Alaska Peninsula (Figure 18d). This distribution of 500-hPa height anomalies is associated with a weak Aleutian low and a negative phase of the PDO.

In summary, the climate regime of positive PDO phase established in the late 1970s appears to have mostly continued, at least in the winter season. On the background of this multidecadal climate regime, there were two minor regime shifts on the decadal time scale. The first shift occurred in 1989 and the second one in 1998, the former being more prominent in winter, whereas the latter in spring-summer. The period 1977-1988 represents a classical positive PDO regime, with a stronger-than-normal Aleutian low and anomalously warm waters along the west coast of North America stretching as far north as the eastern Bering Sea. Variations in the North Pacific climate since 1989 have to do with the north-south pressure dipole in the atmosphere and the second principal SST mode in the ocean, rather than with the PDO phase. During the period 1989-1997, atmospheric pressure tended to be above normal in the high latitudes and below normal in the mid-latitudes, a pattern observed in both winter and spring-summer seasons. This resulted in a relative cooling in the Bering Sea, but no apparent changes in SST variations along the U.S. West Coast were reported. Since 1998, the polarity of the winter north-south pressure dipole reversed. The SST field responded in the way that positive SST anomalies dominated in the eastern Bering Sea, whereas negative SST anomalies were observed along the U.S. West Coast. During the spring-summer season, the 1998 shift exhibited itself in a transition from the north-south pressure dipole to a monopole characteristic of the negative PDO pattern. While there is no strong correlation between winter and summer PDO indices on the year-to-year scale, the two variables experienced similar regime shifts in the past. It is unclear whether the shift in the summer PDO index to significantly negative values from 1999 through 2001 represents just a temporary reprieve from positive PDO conditions, or heralds the onset of an extended period featuring negative PDO conditions throughout the year.

Climate in 2004

After the 2002-2003 El Niño event, El Niño-Southern Oscillation (ENSO) conditions in the equatorial Pacific Ocean remained near-neutral during the first six month of 2004. The Southern Oscillation Index (SOI) shows pronounced month-to-month variability with no persistent positive or negative trend (Figure 20), which suggests a weakening of air-sea coupling in the equatorial Pacific. SST anomalies off the coast of South America (Nino 1+2 region) remain predominantly negative, while in the central equatorial Pacific

(region 3.4, which is considered to be a better indicator of ENSO events) SST anomalies are positive (Figure 21). Based on the latest observations and forecasts from the Climate Prediction Center, it is likely that weak El Nino conditions (with SST anomalies more prominent in the central tropical Pacific) will develop over the rest of 2004 and persist into early 2005.

The mean winter (DJFM) Aleutian low was about 5 hPa deeper than its average value during the 1968-1996 base period. It was also shifted to the northwest of its normal position, a situation conducive to milder than normal winters in the Bering Sea (Rodionov at al. 2004). Cyclonic activity was somewhat enhanced in the Gulf of Alaska. The mean winter 500-hPa anomaly map (not shown) features a north-south dipole over the eastern North Pacific characteristic of positive phases of the EP and Victoria patterns. At the sea level, however, the north-south dipole is much less pronounced.

During the winter of 2004, the SST anomaly pattern in the North Pacific (Figure 22) resembled neither the PDO, nor the Victoria patterns. Winter temperatures were above the 1971-2000 average in the Bering Sea and near the average in the Gulf of Alaska and the U.S. West Coast. The lack of any significant ENSO event in 2004 increases the uncertainty of what major SST pattern should be expected in the winter of 2005.

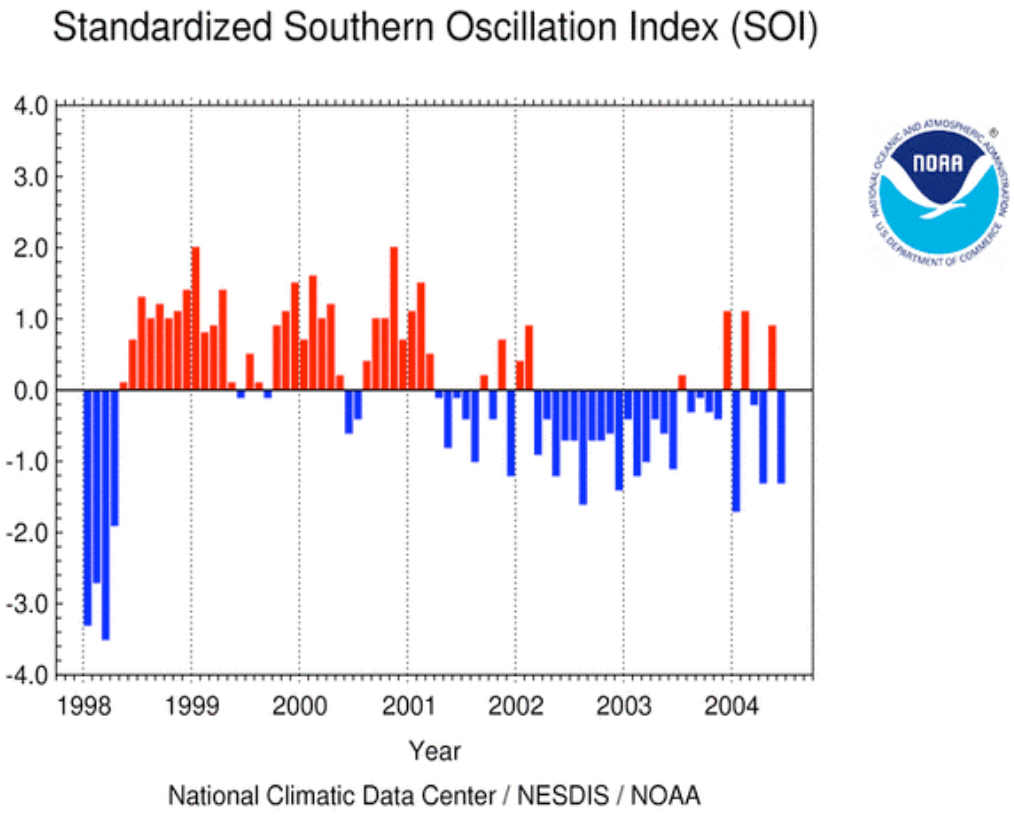

Figure 20. Mean monthly values of the Southern Oscillation Index, January 1998 through June 2004.

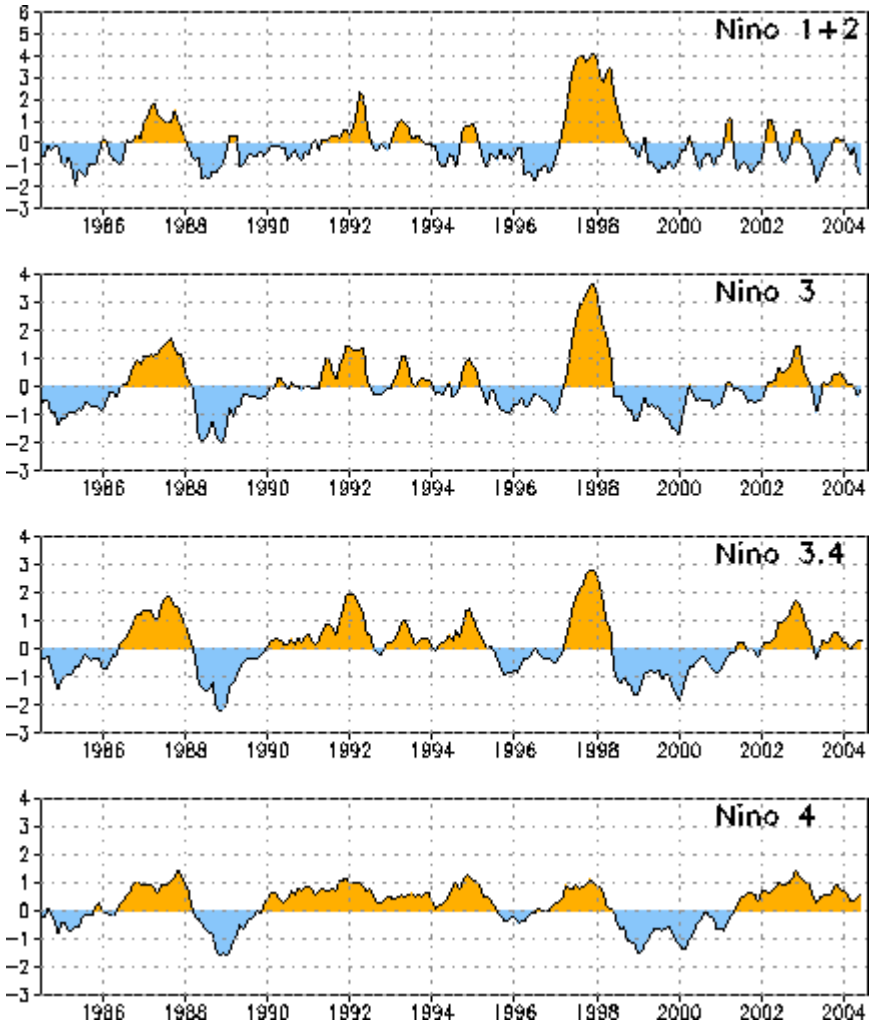

Figure 21. SST anomalies (deg. C) along the west coast of South America (Nino 1+2 region) and central parts of the equatorial belt (Nino 3, 3.4, and 4 regions).

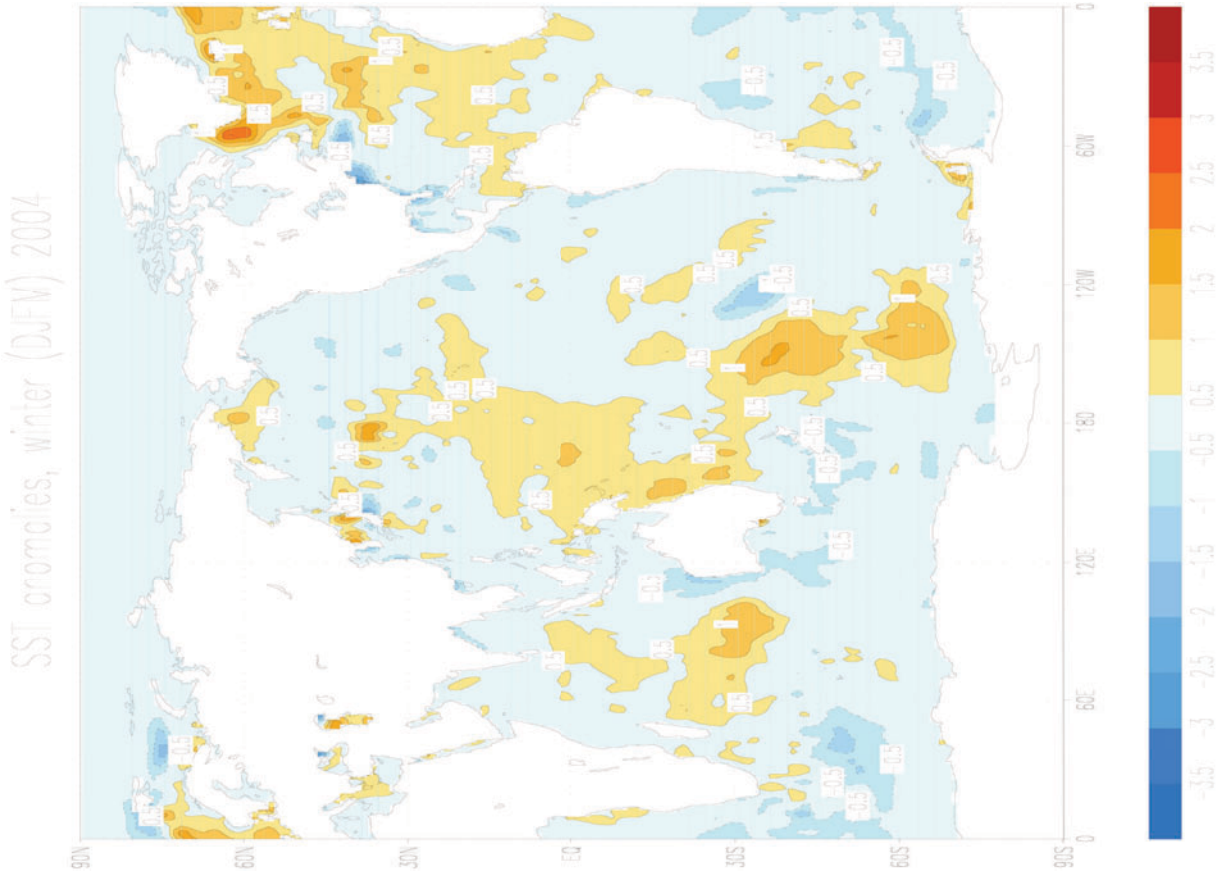

Figure 22. Mean seasonal SST anomalies in the winter (DJFM) of 2004. Anomalies are relative to the 1971-2000 base period. Source data: NOAA OI.v2 SST monthly fields.

GULF OF ALASKA

Pollock Survival Indices –FOCI
Contributed by S. A. Macklin, NOAA/PMEL

Using a conceptual model of early-life survival of western Gulf of Alaska walleye pollock (Megrey et al. 1996) for guidance, FOCI maintains several annual environmental indices. The indices are formulaic elements of a yearly prediction, during the year the fish are spawned, of the number of fish that will recruit as two-year olds. Some indices are determined qualitatively; the two reported here, seasonal rainfall at Kodiak and wind mixing in the exit region of Shelikof Strait, are determined numerically. Although data sources have changed somewhat over the years, chiefly with information used to estimate wind-mixing energy, every effort has been expended to make inter-year comparisons accurate and reliable.

Presently, the FOCI program is developing a modified approach to its annual forecast algorithm. When modifications are complete, it is probable that new indices will become available for this report, while others presented here and in past years may be discontinued. Until a significantly long time series of new annual indices is available, the old indices will continue to be updated and published in this report.

Seasonal rainfall at Kodiak

FOCI uses measured Kodiak rainfall as a proxy for freshwater discharge that promotes formation of baroclinic instabilities (eddies) in the Alaska Coastal Current (ACC) flowing through Shelikof Strait (Megrey et al. 1996). Measured monthly rainfall amounts drive a simple model that produces an index of survival for age-0 walleye pollock. These young fish may benefit from spending their earliest developmental stages within eddies (Schumacher and Stabeno 1994). The model assumes that greater-than-average late winter (January, February, March) precipitation produces a greater snow pack. When the snow melts during spring and summer, it promotes discharge of fresh water through rivers and streams into the ACC. Similarly, greater than average spring and early summer rainfall, with their nearly immediate run-off, also favor increased baroclinity after spawning. Conversely, decreased rainfall is likely detrimental to pollock survival because they do not find the circulation features that promote their survival.

The time series of FOCI's pollock survival index based on measured precipitation is shown in Figure 23. Although there is large interannual variability, a trend toward increased survival potential is apparent from 1962 (the start of the time series) until the mid 1980s. Since then, the survival potential has been more level. Survival potential increased in 2003 and 2004 because almost all winter and spring months experienced average or greater rainfall than their respective 30-year averages. Interestingly, the precipitation-based survival index does not appear to track any of the long-term climate indices, e.g., AO, PDO, with any consistency, possibly because of the way winter and spring precipitation are used in the model. In the 3-yr running mean of the precipitation survival index, there is a change from decreasing to increasing survival potential in 1989. In that year, there was an abrupt shift in the AO.

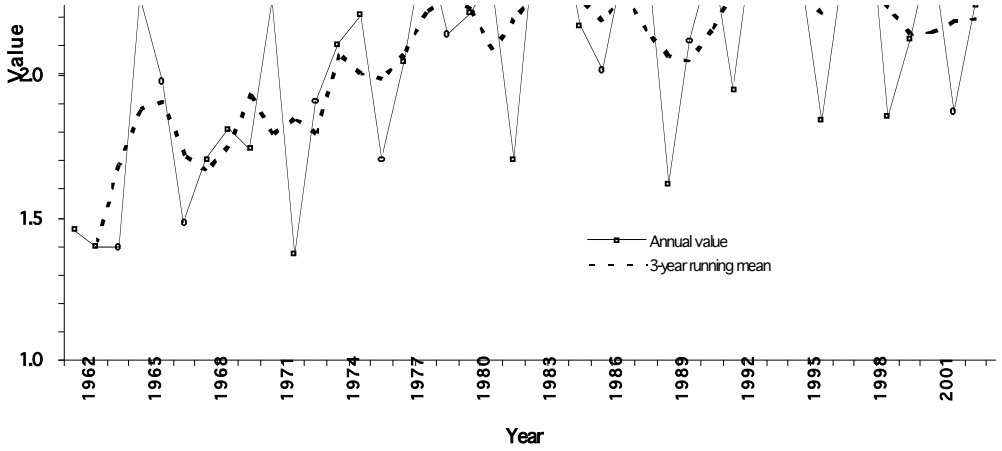

Figure 23. Index of pollock survival potential based on measured precipitation at Kodiak from 1962 through 2004. The solid line shows annual values of the index; the dashed line is the 3-year running mean.

Wind mixing at the southwestern end of Shelikof Strait

Of course, rainfall is only one indicator of early-life-stage pollock survival. FOCI hypothesizes that a series of indices (proxies for environmental conditions, processes and relationships), assembled into a predictive model, provides a method for predicting recruitment of walleye pollock. A time series of wind mixing energy (W m^{-2}) at [57°N, 156°W] near the southern end of Shelikof Strait is the basis for a survival index wherein stronger than average mixing before spawning and weaker than average mixing after spawning favor survival of pollock (Megrey et al. 1996). The wind-mixing index is produced from twice-daily surface winds created from a model (Overland et al. 1980) using NCEP reanalyzed sea-level-pressure fields. The model is tuned to the region using information determined by Macklin et al. (1993). A time series of the wind-mixing index is shown in Figure 24. As with precipitation at Kodiak, there is wide interannual variability with a less noticeable and shorter trend to increasing survival potential from 1962 to the late 1970s. Recent survival potential has been high relative to the early years of the record. Monthly averaged wind mixing in Shelikof Strait generally has been below the 30-year (1962-1991) mean for the last seven January through June periods (1998-2004). This may be further evidence that the North Pacific climate regime has shifted in the past decade.

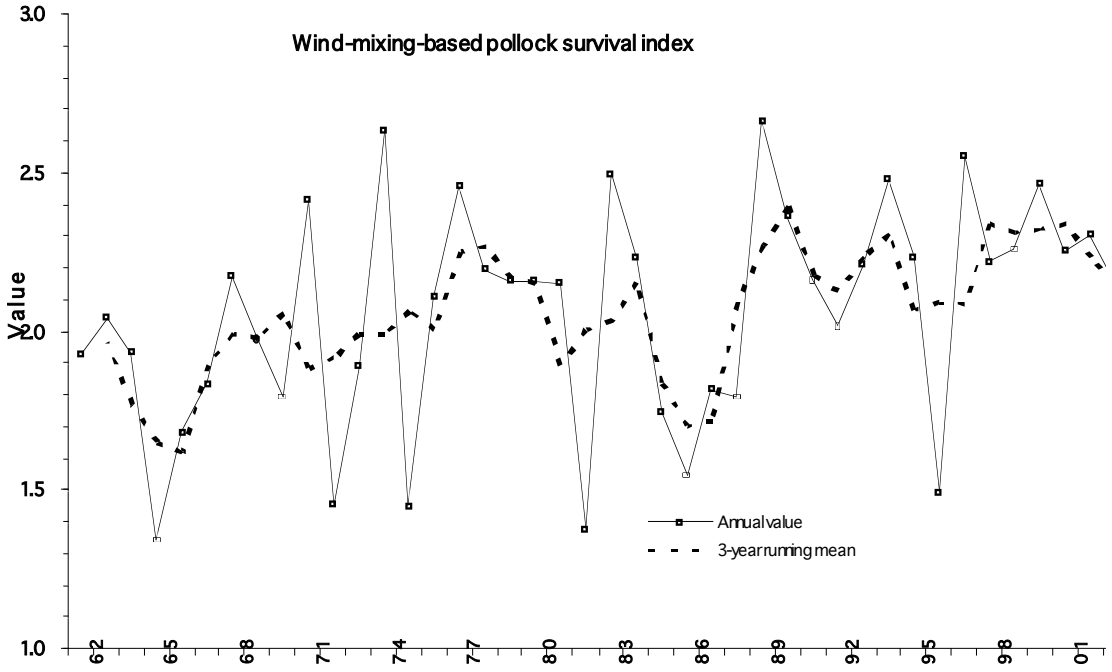

Figure 24. Index of pollock survival potential based on modeled wind mixing energy at [57°N, 156°W] near the southwestern end of Shelikof Strait from 1962 through 2004. The solid line shows annual values of the index; the dashed line is the 3-year running mean.

Ocean transport in the western Gulf of Alaska –FOCI (not updated for 2004)
Contributed by P. J. Stabeno, NOAA/PMEL

The spring and summer seasonal strength of the Alaskan Stream and Alaska Coastal Current (ACC) is an important factor for overall productivity on the shelf of the Gulf of Alaska. FOCI uses satellite-tracked drift buoys, drogued at mid mixed-layer depths (~45 m), to measure ocean currents as a function of time and space. Animations of drifter trajectories from deployments during 2001-2003 can be found at *http://www.pmel.noaa.gov/steller/ssl_drifters.shtml*. There is a strong seasonal signal in the ACC. During late spring and summer, the flow on the Gulf of Alaska shelf between Prince William Sound and the Shumigan Islands is weak. The many bathymetric features such as troughs and banks interact with the currents. This results in flow up the eastern side of such troughs as Amatouli, Chiniak and Barnabas. Flow over banks such as Portlock, is often recirculating, and satellite-tracked drifters can be retained in closed

circulation for weeks to months. ACC flow in the western Gulf of Alaska during 2001 and 2002 was particularly weak. Later in the summer or fall, with the intensification of regional winds, the ACC becomes stronger, and the flow down Shelikof Strait becomes more organized, as shown by the animations for September of 2001 and 2002. During 2003 (Figure 25), ACC flow was more organized and stronger. Specifically, the flow in Shelikof Strait appeared more complex with more meanders and eddies than have been evident in previous years. This year, more than the typical number of drifters went aground along the Alaska Peninsula and the Kenai Peninsula west of Gore Point.

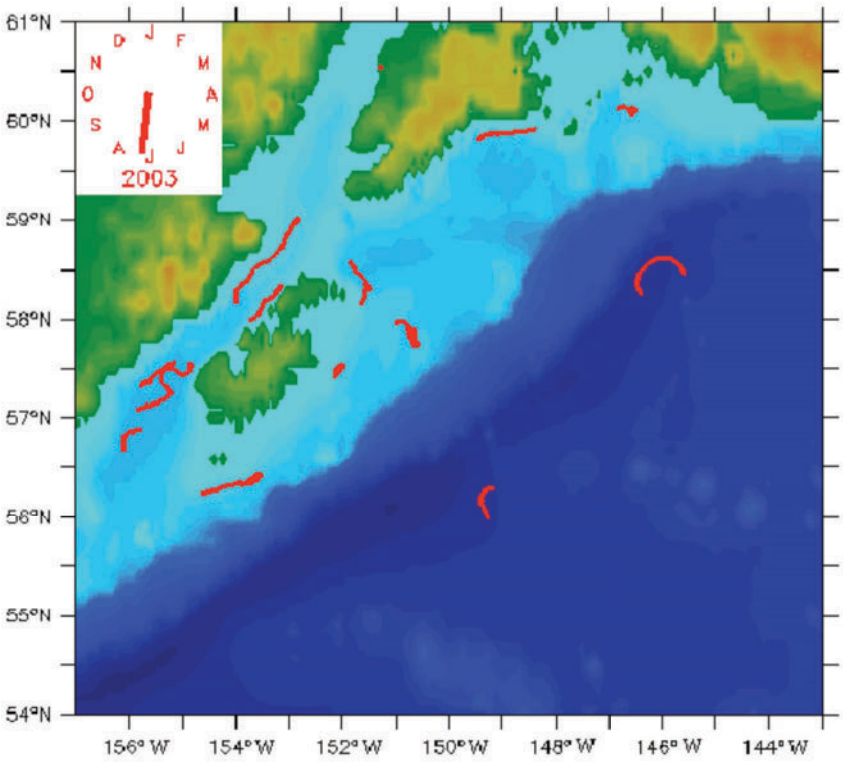

Figure 25. Tracks of satellite-tracked drifters for the period October 14-18, 2001, show sluggish flow on the shelf, except for within Shelikof Strait.

Cross-shelf fluxes are important to providing nutrients to the shelf. Each year (2001-2003) brought flow onto the shelf in the vicinity of the Seward Line, which extends south southeastward from the mouth of Resurrection Bay across the shelf and over the basin. The presence of an eddy is clearly evident from drift trajectories over the basin. Such eddies interact with the shelf, often drawing water off the shelf and into the basin, and are discussed in more detail in the next section. From the head of the gulf to Amchitka Pass, the Alaskan Stream appeared to be fairly typical during 2003, through July, with low eddy kinetic energy and relatively high velocity (>50 cm s^{-1} to the southwest). By next year, there will be enough data to allow construction of an annual Gulf of Alaska transport index that can be compared with climate indices such as PDO, AO, etc.

Eddies in the Gulf of Alaska – FOCI
Contributed by Carol Ladd, NOAA/PMEL

Because the Gulf of Alaska is predominantly a downwelling system, cross-shelf exchange of nutrients is particularly important for productivity on the shelf. Eddies have been implicated as an important mechanism for cross-shelf exchange in the western Gulf of Alaska (Musgrave et al. 1992, Niebauer et al. 1981, Stabeno et al. 2004). The influence of eddies on biological processes has been confirmed with data from the Sea-viewing Wide Field-of-view Sensor (SeaWiFS) showing elevated chlorophyll associated with eddies.

Eddies propagating along the slope in the northern and western Gulf of Alaska are generally formed in the eastern gulf in the autumn or early winter (Okkonen et al. 2001). In most years, these eddies impinge on the shelf east of Kodiak Island in the spring. Using altimetry data from 1993 to 2001, Okkonen et al. (2003) find an eddy in that location in the spring of every year except 1998. They find that strong, persistent Yakutat eddies occur more often after 1997 than in the period from 1993 to 1997.

In the spring/summer of 2004, two eddies were located near the Kodiak Island shelf: one northeast of Kodiak Island and one south of the island near the exit of Shelikof Strait (Figure 26). The southernmost eddy was formed in the winter of 2003, while its more northern counterpart was formed in winter of 2004. In situ observations of water properties within these eddies suggest that the eddies trap shelf water in their interior and transport it off-shelf into the basin. This eddy core is likely to contain shelf-derived species of zooplankton and concentrations of iron and other nutrients, as has been found for Haida eddies, found farther south in the Gulf of Alaska (Mackas and Galbraith 2002, Whitney and Robert 2002). The eddy core of the 2003 eddy was observed to maintain its coastal signature through at least May 2004.

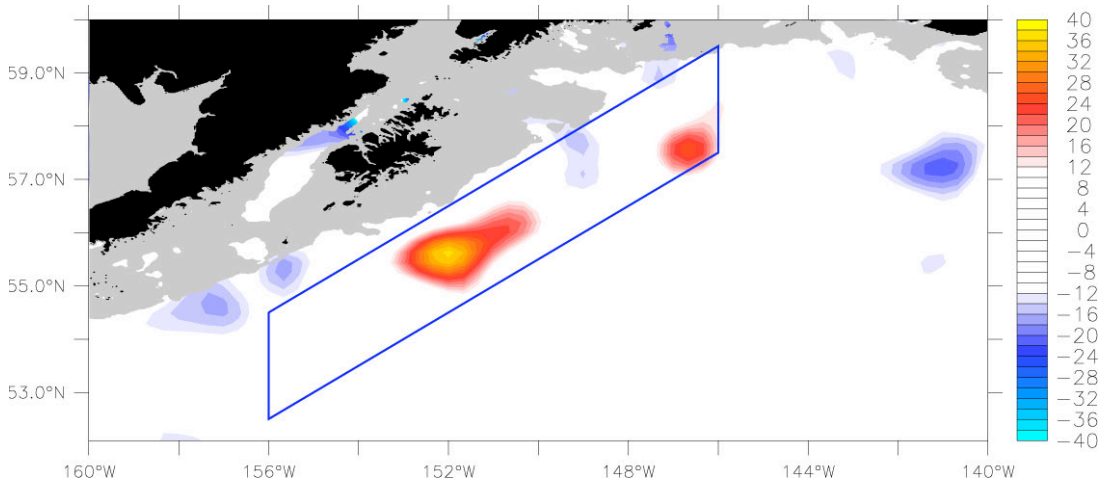

Figure 26. Sea surface height anomaly from TOPEX/Poseidon, ERS-1/2 and Jason merged altimetry. Positive anomalies imply anticyclonic circulation. Blue line outlines region over which EKE was averaged for Figure 27.

Since 1992, the Topex/Poseidon satellite altimetry system has been monitoring sea surface height (SSH). Gridded altimetry data (merged TOPEX/Poseidon, ERS-1/2 and Jason at 1/3 degree resolution; Ducet et al. 2000) was used to obtain an index of energy associated with eddies in the Gulf of Alaska. Figure 27 shows a time series of eddy kinetic energy (EKE) in the region where eddies often impinge on the shelf near Kodiak Island (see Figure 26 for region over which EKE was averaged). EKE during the first half of 2004 was high compared to the rest of the record, probably because two eddies were active in the region. Prior to 2000, EKE was generally lower than the ~11-year average, although 1993 and 1997 both showed periods of high EKE. In addition, the amplitude of the quasi-seasonal cycle also appears to have increased later in the record. Research is ongoing on the causes and implications of these patterns. (The altimeter products were produced by the CLS Space Oceanography Division as part of the Environment and Climate EU ENACT project [EVK2-CT2001-00117] and with support from CNES; downloaded from http://www.aviso.oceanobs.com/).

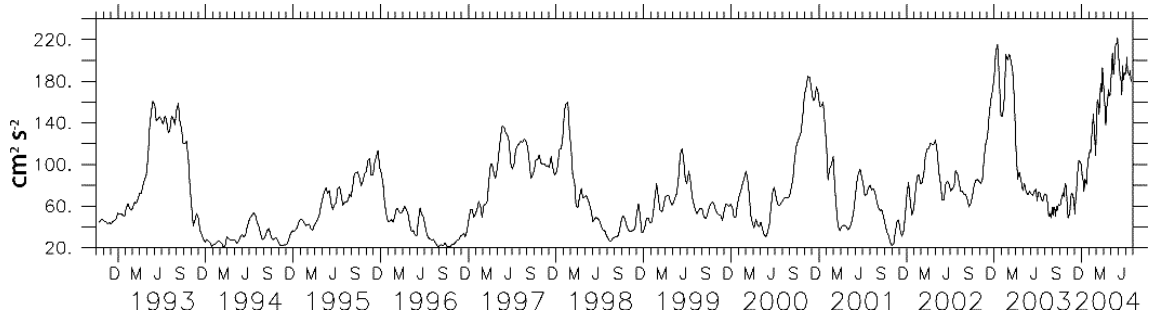

Figure 27. Eddy kinetic energy averaged over the region shown in Figure 26 calculated from TOPEX/Poseidon, ERS-1/2 and Jason-merged altimetry.

EASTERN BERING SEA - 2004

Temperature and Ice Cover –FOCI

S. Rodionov, J. Overland, P. Stabeno, N. Bond, and S. Salo, NOAA/PMEL

Summary. *The very warm winters of the late 1970s and 1980s were followed by cooler winters in the 1990s. This cooling was likely a result of a shift in the Arctic Oscillation and hence a tendency for higher sea-level pressure (SLP) over the Bering Sea. Since 1998, negative SLP anomalies have prevailed, which is indicative of greater Pacific influence and consistent with generally milder winters. The winter of 2004 was anomalously warm (although somewhat colder than the winter of 2003), with temperatures typical of the first decade after the 1977 regime shift. Ice cover in the vicinity of Mooring 2 was below the 1989-2004 average almost all season long, except during a cold spell in late March-early April. Spring air and sea surface temperatures were much above normal.*

The winter of 2004 in the Bering Sea was mild, with mean winter (DJFM) surface air temperature (SAT) at St. Paul of 1.34°C above the 1961-2000 average. Such mild winters are typical for the post-1977 climate regime, particularly during its first decade (Figure 33a). The shift of 1977 was very sharp, from the near record cold winters of 1975 and 1976 to the near record warm winter of 1979. This shift to a warmer climate and the previous shift to a colder climate in the late 1930s can be detected using the STARS change detection method (Rodionov 2004) at the confidence level $p < 0.01$. At the less strict confidence level of 0.2, the relatively cold period 1990-2000 can be singled out (Figure 33a). Of these 11 winters, only one winter (1996) was anomalously warm; all other winters were either near or below the 1961-2000 average. This cooling is a manifestation of the decadal-scale climatic variations that occur on the background of multi-decadal climatic regimes (see climate overview for the North Pacific).

The SAT at St. Paul during spring has been generally warm since the late 1970s regime shift (Figure 33b). During the last three spring seasons (2002-2004), SAT anomalies at St. Paul were greater than 1.7˚C (relatively to the 1961-2000 base period), which is anomalously warm even for the post-1977 regime. Note that apart from a relatively short warm period in the late 1930s, spring SAT anomalies were predominantly negative from the beginning of the record in 1916 until the regime shift in 1977.

Warm (cold) winter climatic regimes in the eastern Bering Sea tend to be associated with the periods of anomalous low (high) SLP, as expressed by the Bering Sea pressure index (BSPI), although the timing of the shifts in the winter SAT and BSPI may not be exactly in the same years (cf. Figures 33a and 33c). The BSPI is a measure of an overall cyclonic activity in the region and is closely linked with the strength of the Aleutian low. It is important to note that on the year-to-year scale the correlation between the BSPI and winter SAT at St. Paul is week (r = -0.16 for the 1978-2004 period). The reason is that winter climatic conditions in the Bering Sea depend not as much on the strength of the Aleutian low, as on its geographical position (Rodionov et al. 2004). On the multidecadal time scale, anticyclonic anomalies over the Bering Sea reflect the increased Arctic

influence on the sea, whereas cyclonic anomalies characterize the increased Pacific influence. Thus a shift of 1977 from a cold to warm multidecadal regime was associated with an abrupt intensification of cyclonic activity over the North Pacific in general and the Bering Sea in particular. During the relatively cold period in the 1990s the BSPI was mostly near or above the 1961-2000 average (Figure 33c). Since 1998, cyclonic activity in the region intensified again. There was no winter during this later period (1998-2004) when the BSPI was positive. The average BSPI value for this 7-year period was the lowest for any consecutive 7-year period since the record began in 1900.

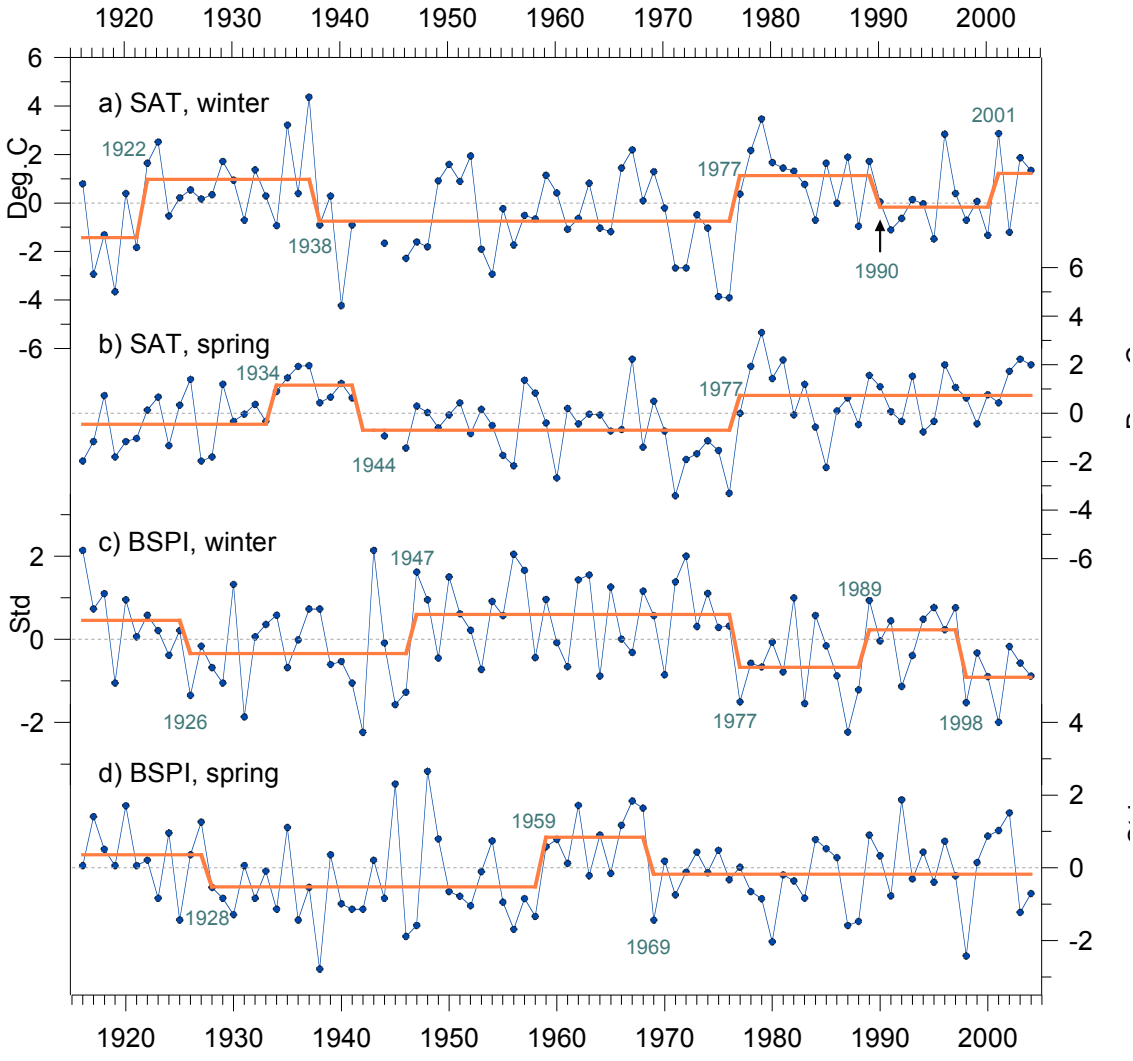

Figure 33. a) Mean winter and b) spring surface air temperature anomalies in St. Paul, Pribilof Islands, c) winter and d) spring Bering Sea pressure index. The winter months are December through March and spring months are April through June. The base period for calculating anomalies is 1961-2000. The stepwise functions (orange lines) characterize regime shifts in the level of fluctuations of the variables. Shift points were calculated using the STARS method (Rodionov 2004), with the cutoff length of 10 years and significance level of 0.2.

The spring BSPI (Figure 33d) tended to be negative during the period 1978-1989 and positive since 1990, but the difference between these two periods was not significant enough to qualify as a regime shift. There is no strong correlation between the BSPI and SAT at St. Paul in spring on the interannual time scale. Nor there are any similarities between these two variables in terms of regime shifts. The relationship between atmospheric pressure and thermal conditions in the Bering Sea is more complex in spring than in winter because the dynamic and radiative factors become comparable. When higher-pressure is present over the Bering Sea, there is often also a relatively cold low-level air mass. But it also means lighter winds, less cloud cover, more solar insolation, and hence, greater radiative heating of the ocean. Similarly, anomalously low SLP implies a trade-off between the advection of warm Pacific air and more clouds and hence less solar insolation.

Variability in ice cover in the Bering Sea depends on both temperature and atmospheric circulation. In turn, sea ice has a profound influence on the physical and biological ocean environment. Prior the climate shift in the late 1970s, the ice cover index (ICI) was predominantly positive (Figure 34a). After the regime shift, the winters from 1978 through 1989 were particularly mild. During this 12-year period there were only three winters when the ICI was slightly positive. During a relative cooling in the 1990s, the frequency of winters with above normal ice cover increased (8 winters with positive versus only 3 winters with negative ICI values during the period 1990-2000). The more recent winters were very mild again, particularly in 2001, 2003, and 2004 (Overland and Stabeno 2004).

As Figure 34b illustrates, there is a clear overall downward trend in the ice retreat index (IRI). Since the early 1970s, the index is declining at an average rate of almost 1 day per year, a trend significant at the 95% level. The IRI represents the number of days with ice cover after March 15 in the 2˚ x 2˚ box (56-58°N, 163-165°W) that includes Mooring 2 (57^{o}N, 164^{o}W). Based on the 1973-2004 statistics, the ice usually retreats from this area in the second week of April. During the period 1996-2004, there was only one year (1999) when ice stayed in the vicinity of Mooring 2 after that date. In the late 1990s, the early ice retreat was compensated by its early arrival, and the length of the ice season was near its average value of 85 days. In more recent years, the length of the ice season significantly shortened. Based on ice melt and changes in atmospheric circulation patterns, Stabeno and Overland (2001) report the Bering Sea is shifting to an earlier spring transition. In the winter of 2004, ice cover in the vicinity of Mooring 2 was below the 1989-2004 average almost the entire season, except for a brief cold spell in the end of March and early April (Figure 35).

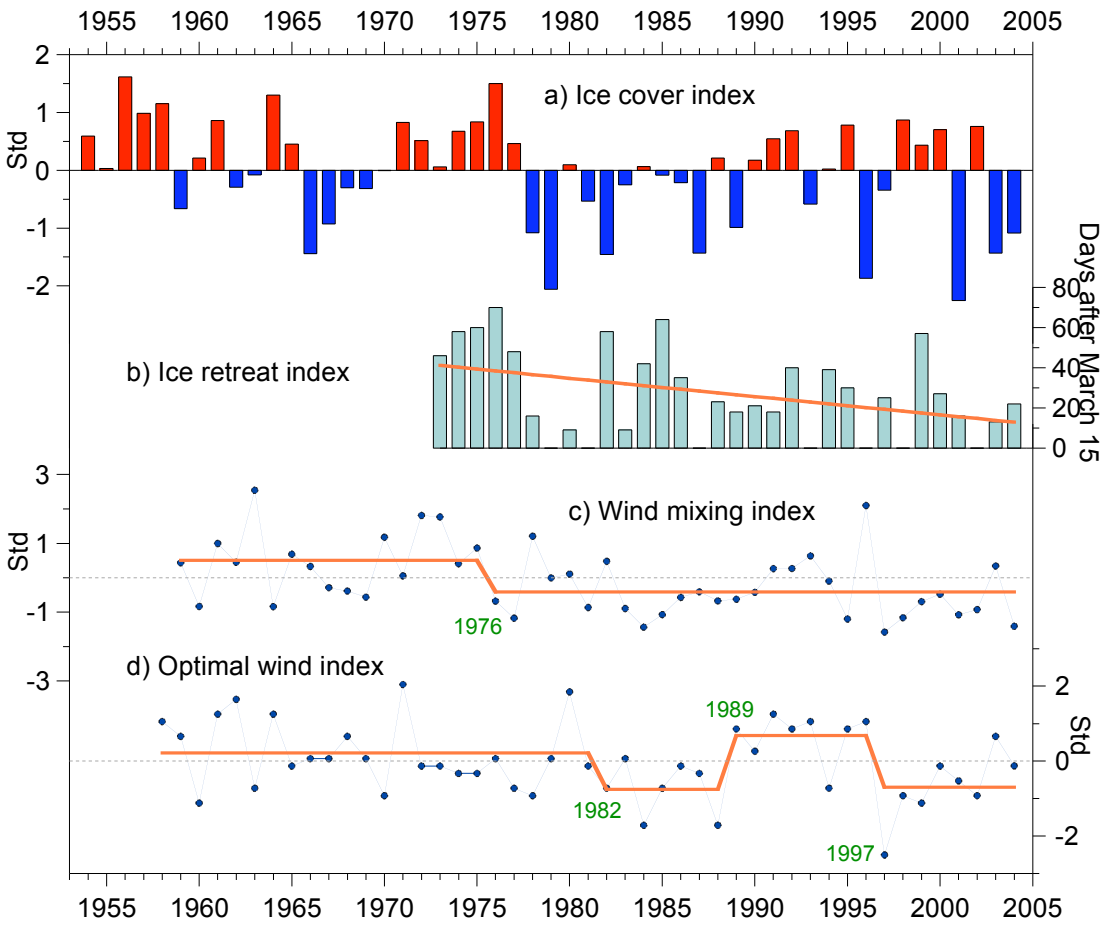

Figure 34. a) Ice cover index, 1954-2004, b) ice retreat index and its linear trend (orange line), 1973-2004, c) wind mixing index (June-July) at Mooring 2, 1959-2004, and d) optimal wind index for successful larval feeding (1 May – 15 July), 1958-2004. The stepwise functions (orange lines) characterize regime shifts in the level of fluctuations of the variables. Shift points were calculated using the STARS method (Rodionov 2004), with the cutoff length of 7 years and significance level of 0.2.

Sea surface temperatures in May, after ice has retreated from the southeastern Bering Sea, appears to be, to a large extent, a product of processes operating during the previous winter. For example, the MaySST index (average SST over the SE Bering Sea) is significantly correlated with winter indices such as the ICI, $r = 0.50$ ($P < 0.05$), and winter surface air temperature in St. Paul, $r = 0.59$ ($P < 0.01$), for the period 1970-2003. The MaySST index is also a good predictor for the summer bottom temperature as illustrated in Figure 36. The correlation coefficient between these two variables is $r = 0.82$ ($P < 0.001$) for the period 1982-2003. In 1999, the MaySST index reached the record low value since the beginning of observations in 1970. Since then this index has increased steadily. Due to the very mild winter and spring of 2003, the MaySST index in that year reached the highest value since 1981. Mean May SST in 2004 remained well above normal.

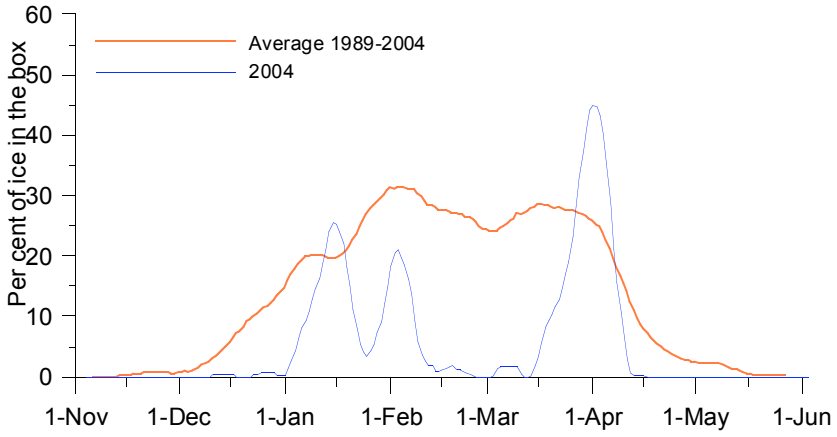

Figure 35. Percentage of ice cover in the 2˚ x 2˚ box (56-58°N, 163-165°W) during the winter of 2004.

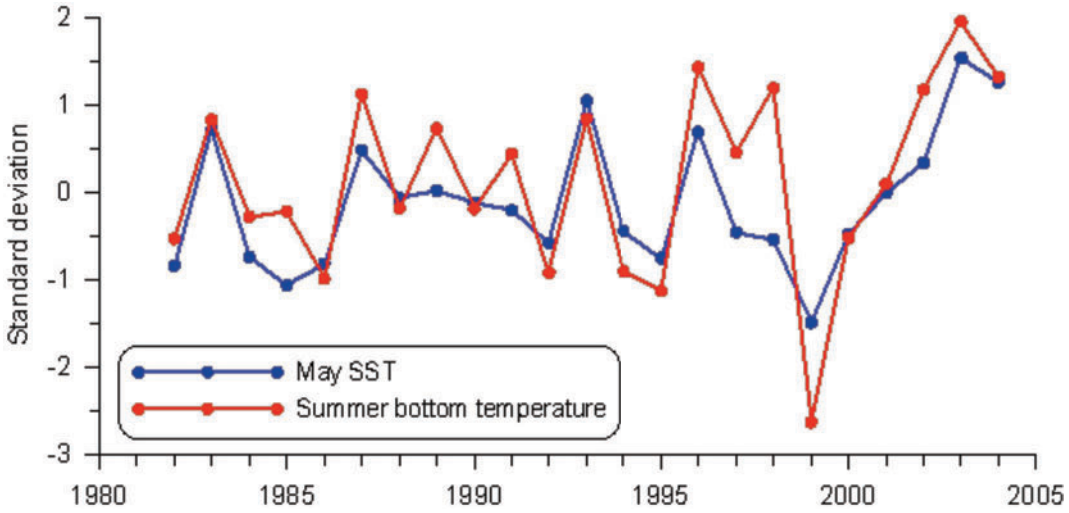

Figure 36. The May SST index (derived from NCEP/NCAR Reanalysis project) and mean summer bottom temperature (from bottom trawl surveys) in the southeastern Bering Sea.

Two indices were chosen to characterize wind conditions in the Bering Sea. The wind mixing u^{*3} at Mooring 2 provides a good measure of warm season storminess. The quantity u^{*3} represents the rate at which turbulent energy is supplied to the ocean by the winds, and ultimately relates to the rate of mixing at the base of the upper mixed layer. This exchange can be important to the ecosystem because it represents a mechanism for the transfer of nutrients from water below the pycnocline into the euphotic zone. This mechanism appears to be important in early summer over the Bering Sea shelf, through its role in sustaining primary production after the spring bloom. Figure 34c shows that during the warm climate regime since the late 1970s (and particularly since 1983) the wind mixing index tends to be negative. One prominent exception was the summer of 1996, which was very windy. As the observations at Mooring 2 indicate, that summer

featured a thicker upper mixed layer, a weaker thermocline, and sustained primary productivity relative to the other years (Stabeno et al. 2001). It should be noted that

The second wind-related index tracks wind speeds favorable for successful larval feeding. Formally, it refers to the number of days each year during the period 1 May through 15 July in which the daily average wind speed was in the range 4.8 to 9.5 ms^{-1} at the location of Mooring 2. It is based on the study of Megrey and Hinckley (2001), which used a process oriented individual-based model (IBM) of walleye pollock larvae to evaluate the influence of wind-generated turbulence on feeding. Feeding success depends on turbulence through the latter's effects on the rate at which pollock larvae would encounter prey. The time series of the optimal wind index (Figure 34d) shows that there were relatively high number of optimal wind speed days during the period 1989-1996, while the periods 1982-1988 and 1997-2002 stand out as having low frequencies of wind speeds in this optimal range.

In summary, the main characteristic of the Bering Sea climatic conditions in the last 4 years is a year-to-year persistence in lack of sea ice, warm bottom temperatures, and warm air temperature anomalies in late winter through summer, even though the Arctic Oscillation and Pacific Decadal Oscillation indices have shown large interannual variability. Bering Sea indicators should be watched closely over the next 5 years to see whether the ecosystem is experiencing a substantial biogeographical shift northward in response to changing temperature and atmospheric forcing (Overland and Stabeno 2004). If this shift continues over the next decade, it will have major impacts on commercial and subsistence harvests as Arctic species are displaced by sub-Arctic species.

Simulated Drift Trajectories in the Southeast Bering Sea –FOCI
Contributed by Dylan Righi, FOCI, NOAA/PMEL

One of the most important resources in the Bering Sea (both for economic value and for its role in the ocean ecosystem) is the walleye pollock (*Theragra chalcogramma*) fishery. In the 1998, 50% of the world ocean catch of pollock came from the Bering Sea (Napp et al. 2000). At the same time walleye pollock (especially juveniles) are the main prey of other fishes, seabirds and marine mammals, meaning changes in stock size exert pressure on the entire Bering Sea food web. There are large inter-annual variations in pollock recruitment (Wespestad 1993) that must be understood in order to successfully manage this fishery. Climate variability and physical forcing play an important role in recruitment of fish and shellfish species (Wespestad et al. 2000; Wilderbuer et al. 2002; Zheng and Kruse 2000). Pollock recruitment is understood to be mainly set by their first year (Kendall and Duker 1998) and one fate that young pollock meet is cannibalism by adult pollock. Thus, transport of pollock eggs and larvae to regions of high adult density should adversely affect survival. Wespestad et al. (2000) test this hypothesis by using a surface transport model (OSCURS, (Ingraham and Miyahara 1988)) to simulate egg/larvae trajectories, and hindcasting survival rates. We attempt to improve on this work by using a full primitive equation ocean model to calculate trajectories instead.

We have used the northeastern Pacific Regional Ocean Model System (ROMS) to simulate trajectories in the southeastern Bering Sea. Drifter tracking in ROMS is done using a fourth order predictor-corrector scheme and allows vertical movement. We currently have results for the years 1996-2003. The simulated drifters are initialized in the Bering Sea just north of Unimak Island and to the northeast of Unimak Pass. This is known to be an area of spawning for walleye pollock (Hinckley 1987). The initial drifter positions fill out a seven by seven grid with horizontal separations of about 10 km (Figure 37). Vertically, there are 15 drifters initialized at each grid point with maximum depths just over 40 m. The drifter initial positions are denser near the surface, replicating vertical egg distribution data collected in the Bering Sea (Kendall et al. 1994). Drifters are released on April 1 of each year and are tracked for 90 days.

Endpoints after 90 days for drifter trajectories from the 1998-2003 runs are shown in Figure 38 (this plot shows all drifters at all depths). In all years there is a strong tendency for trajectories to move to the northeast up the Alaskan peninsula. The other common path is movement to the northwest along the 100-m isobath. The split between these two paths is seen clearly in the 1998, 1999, 2001 and 2003 drifter endpoints. The full trajectory plots (not shown here) show that the endpoints in 2000 are the result of a strong turning to the northwest of trajectories that had been moving up the Alaskan peninsula. In 2002 the drifters initialized at deeper points follow the common paths along the peninsula and the 100-m isobath. But drifters nearer the surface seem influenced by local winds and first move to the northeast, then turn to the northwest, resulting in endpoints spread evenly across the entire shelf. Further study of possible forcing mechanisms is needed to understand what leads to these years departing from the archetypal two-limbed flow.

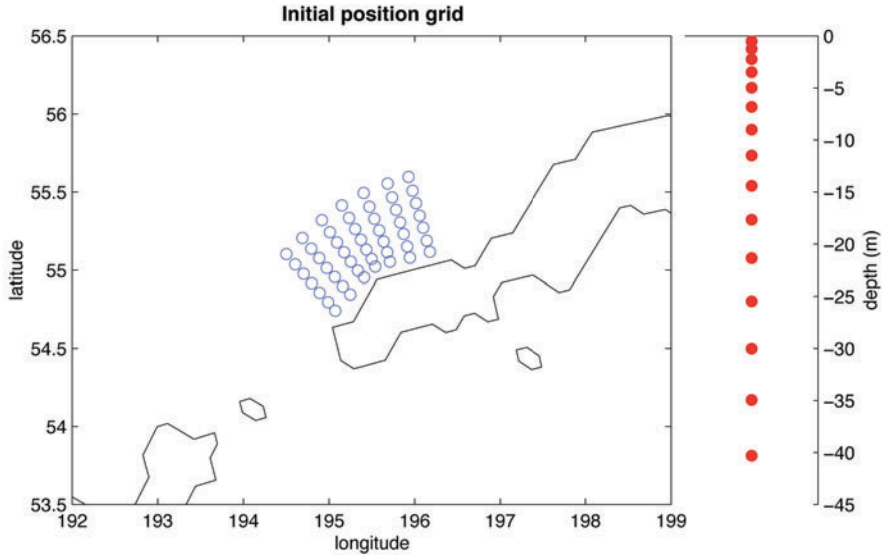

Figure 37. Simulated drifter initial horizontal (left) and vertical (right) positions.

The initial goal of this work was to compare simulated trajectories from a full primitive equation model with those from the Ocean Surface Current Simulations (OSCURS) numerical model. OSCURS computes daily surface current fields using daily sea level

pressure and long-term mean geostrophic current data. As such, it is a simpler model in terms of the physics involved but is much more computationally inexpensive. Wespestad et. al. (2000) used OSCURS to create simulated trajectories in the Bering Sea. The initial grid used here was centered on the initial release point they used. Our trajectories for drifters released near the surface (0 to 5 m depth) show good agreement with the OSCURS results. But our results show variation of trajectory endpoints with changes in both horizontal and vertical initial position. Figure 39 shows the full trajectories for the 2001 simulated drifters. The upper left panel shows the tracks of all the drifters released, while the upper right and the bottom panels show drifter tracks as a function of their release depth. Within each depth bin it is evident that there is a large dependence of drifter endpoints on initial vertical placement with each bin showing, to relative degrees, the two-limbed split flow.

There is also a strong dependence on release depth. The OSCURS 2001 trajectory (not presented here) moves a short distance to the northeast up the Alaskan peninsula as do the majority of the NEPROMS drifters released in the upper 5 m of the water column (upper right panel of Figure 39). But with deeper release points comes a stronger divergence of the trajectory fates. In the 5-20 m and 20-40 m release bins there are significant numbers of drifters that join the 100-m isobath flow to the northwest, with some even moving through Unimak Pass before turning back. OSCURS results would completely miss this variation in particle fates.

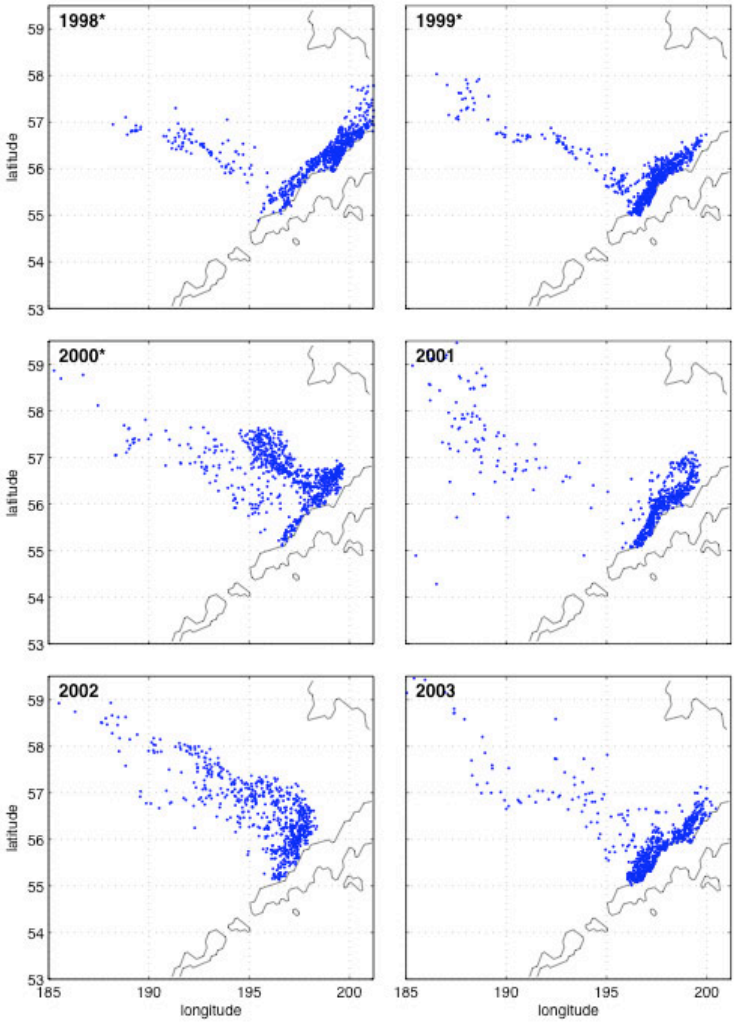

Figure 38. Endpoints for 90-day drifter trajectories for 1998-2003.

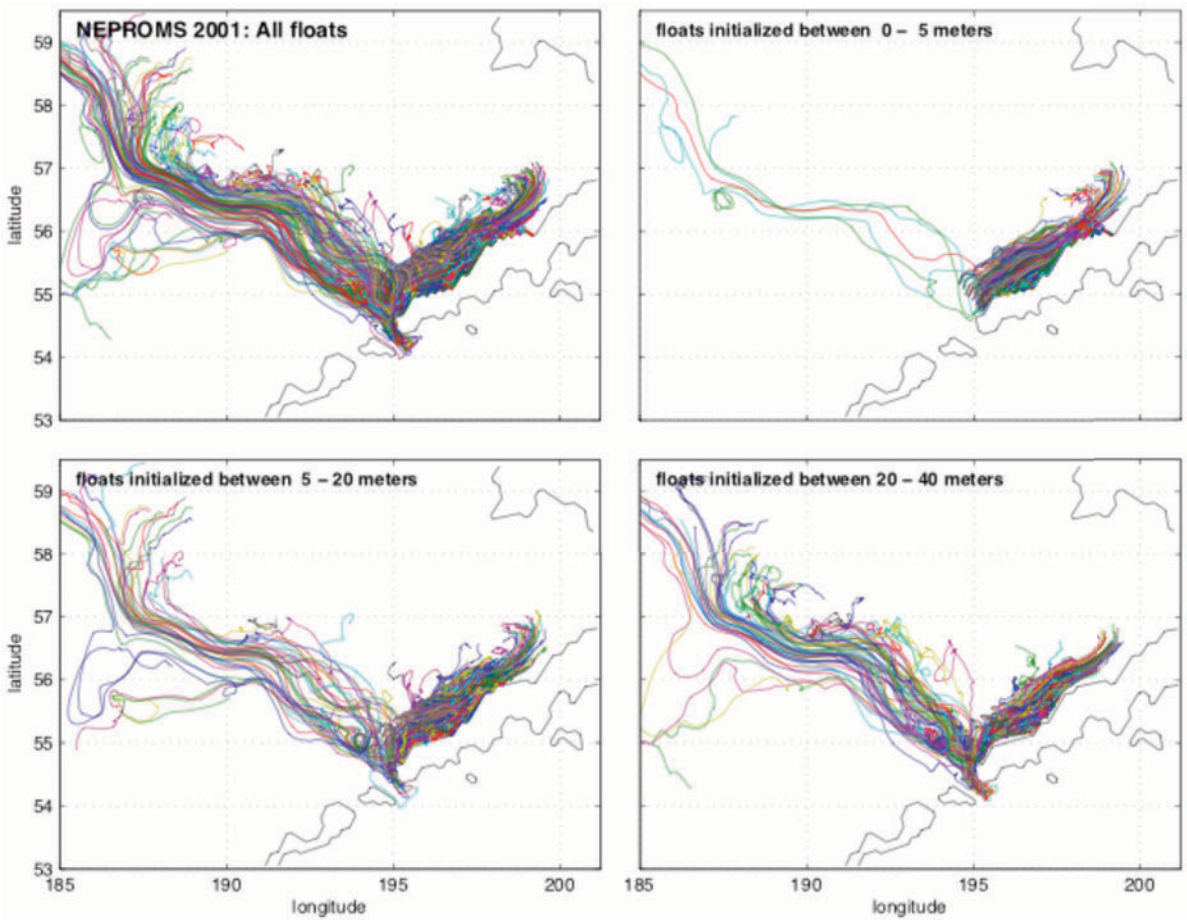

Figure 39. Full trajectories for the 2001 90-day simulated drifters. Upper left panel shows all drifters, while the upper left and bottom panels show drifters divided as a function of initial release depth.